removed and recombinant human PlGF (rhPlGF) solution (10 ng/100 µl in 100 mM NaCl, 50

mM Tris, 20m M imidazole, and 0.1 mg/ml BSA) was added to the precipitate, which included

the Ni-agarose-rhsFlt-1 complex, and incubated overnight at 4°C. After centrifugation to

remove the Ni-agarose-rhsFlt-1 complex bound to rhPlGF, the uncombined rhPlGF in the

supernatant was measured by ELISA, which confirmed that rhsFlt-1 bound rhPlGF in a

dose-dependent manner (Supplementary Figure 3C). We next used ELISA to measure serum

hsFlt-1 levels and free mouse PlGF-2 30 min after intraperitoneal administration of rhsFlt-1 to

wild-type C57BL/6 mice (15 ng/g BW) to confirm that the injected rhsFlt-1 binds to

endogenous mouse PlGF-2. After injection of rhsFlt-1, serum rhsFlt-1 increased to 3957 ±

916 pg/ml (Supplementary Figure 3D), and levels of endogenous mouse PlGF-2 were

significantly reduced, as compared to control (PBS) (8.1 ± 1.4 vs. 13.7 ± 0.8 pg/ml; n=9, 8; P

<0.01, Supplementary Figure 3E). The serum concentration of endogenous VEGF tended to

be lower in mice treated with rhsFlt-1 than in mice treated with PBS, but the difference was not

statistically significant (58.1 ± 1.8 vs. 66.6 ± 8.4 pg/ml; n=9, 8; P =0.308).

Physical Examination. Blood pressures and heart rates were measured once every 2

weeks using a tail-cuff system (BP-98A; Softron) that utilizes a photoelectric sensor to detect

blood flow in the tail (2). The mice were familiarized to the procedure before they were 12

weeks old (Supplementary Figure 4).

Supplementary Figure 1

Plasma sFlt-1 levels and the relationship between plasma sFlt-1 and PlGF levels and coronary atherosclerosis. (A) Plasma levels of sFlt-1 from the renal vein were the highest among those from aorta, coronary sinus (CS), hepatic vein, and renal vein. *n=14*. *$P<0.05$. (B) Plasma levels of sFlt-1 from aorta were positively correlated with plasma levels of sFlt-1 from renal vein. *n=126*. r=0.70. $P<0.001$. (C, D) When dividing patients into 5 groups according to renal function as described in supplemental method, the extent of coronary atherosclerosis in terms of both the number of coronary arteries showing >75% stenosis (C) and Gensini's score (D) in CKD patients was severer in patients with more severe renal dysfunction. *n=329*. *$P<0.05$ vs. Group1 in C and D. sFlt-1 (E) and PlGF (F) in patients without coronary stenosis and in those with 1-, 2-, and 3-vessel disease. sFlt-1 tended to be lower and PlGF tended to be higher in accordance with coronary atherosclerosis severity, but neither difference reached the level of statistical significance. Data are means ± SEM.

Supplementary Figure 2

(A-B) Plasma levels of PlGF (A) and serum levels of VEGF (B) in samples collected from the aorta. Both values did not have significant correlation with eGFR. *n=314*. r=0.00. $P=0.991$.(A) *n=325*. r=0.10. $P=0.079$.(B) (C-D) Plasma PlGF levels (C) or serum VEGF levels (D) in

samples from aorta, CS, hepatic vein, and renal vein. PlGF levels did not significantly differ among these vessels. Serum levels of VEGF from hepatic vein were higher than those from renal vein, but not those from aorta or CS. $n = 14$. *$P < 0.05$. (E-F) VEGF/sFlt-1 ratios plotted against renal function (E) and extent of atherosclerosis (F). VEGF/sFlt-1 ratios showed no significant relationship with eGFR (r= -0.10. P=0.073) and no tendency to differ according to the number of diseased coronary vessels. Data are means ± SEM.

Supplementary Figure 3

Validities of the specific primers for sFlt-1 and recombinant human sFlt-1 (rhsFlt-1). (A) Extracted mRNA from renal biopsy specimens was tested to confirm the specificity of the primer for human sFlt-1. Extracted mRNA from human umbilical endothelial cell (HUVEC) was used as a positive control at 4 graded concentrations. A single PCR product was observed in a dose dependent manner and a single band was also detected in patient's sample (Pt). (B) The PCR for human sFlt-1 did not cross-react with full length human Flt-1. In lanes 1 and 3, PCR products were amplified using full length Flt-1 cDNA as a template, in lanes 2 and 4, PCR products were amplified using sFlt-1 cDNA as a template. Lanes 1 and 2 were amplified using specific primers for full length Flt-1, lanes 3 and 4 were amplified using specific primer for sFlt-1. M stands for marker. (C-E) The efficacy of recombinant human sFlt-1 (rhsFlt-1) was
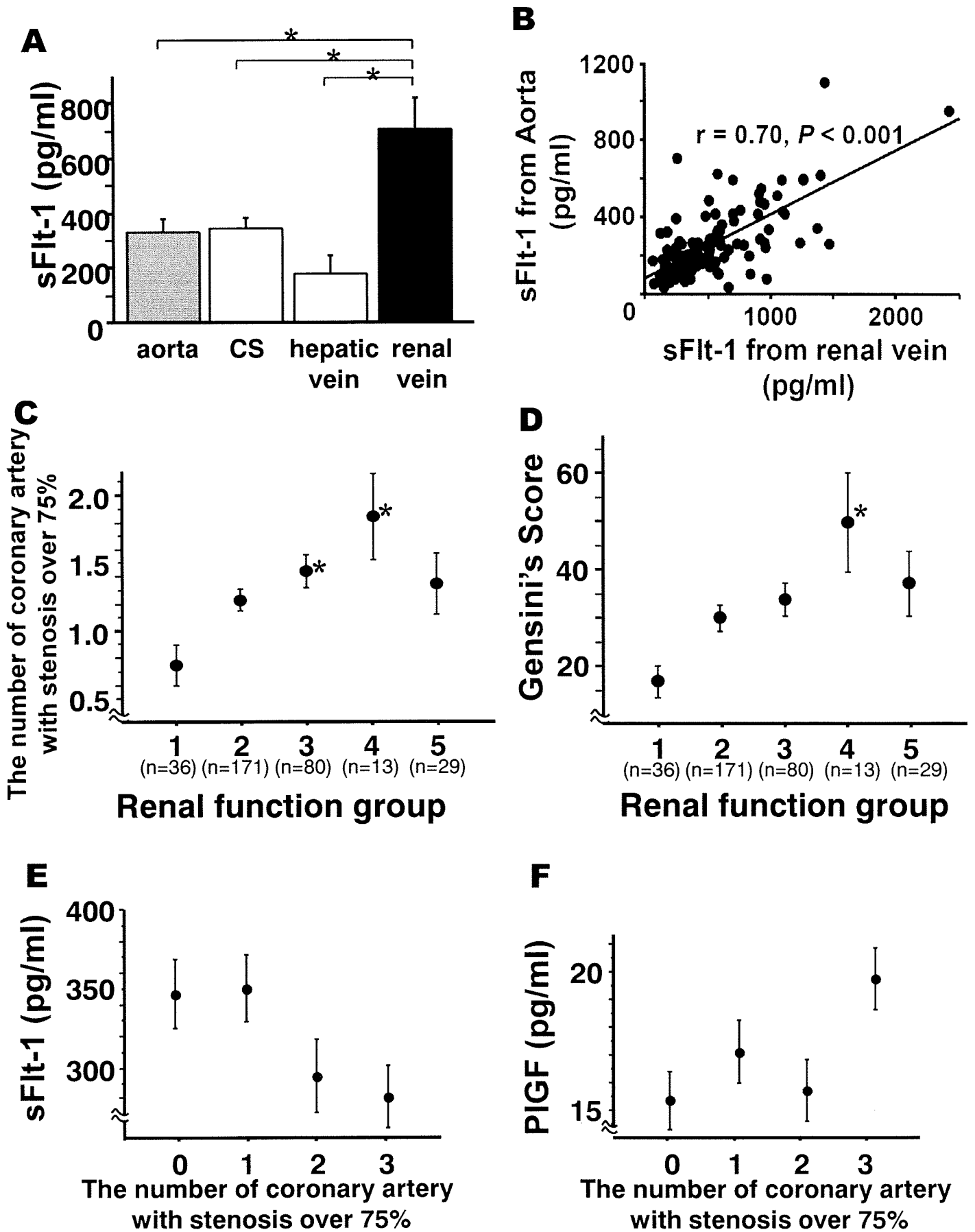
confirmed by demonstrating that it bound PlGF *in vitro* and *in vivo*. (C) When recombinant human PlGF (0.32 pM) was incubated with six different concentrations of rhsFlt-1 (0 to 100 pM), rhsFlt-1 bound to rhPlGF in a dose dependent manner. (D-E) Serum levels of human sFlt-1 and free mouse PlGF-2 were measured 30 min after intraperitoneal administration of rhsFlt-1 (15 ng/g BW) or PBS to wild-type C57/BL6 mice. (D) Human sFlt-1 was not detected in control mice. (E) Serum levels of mouse PlGF-2 were significantly reduced in rhsFlt-1-injected mice. $**P < 0.01$. Data are means $\pm$ SEM.
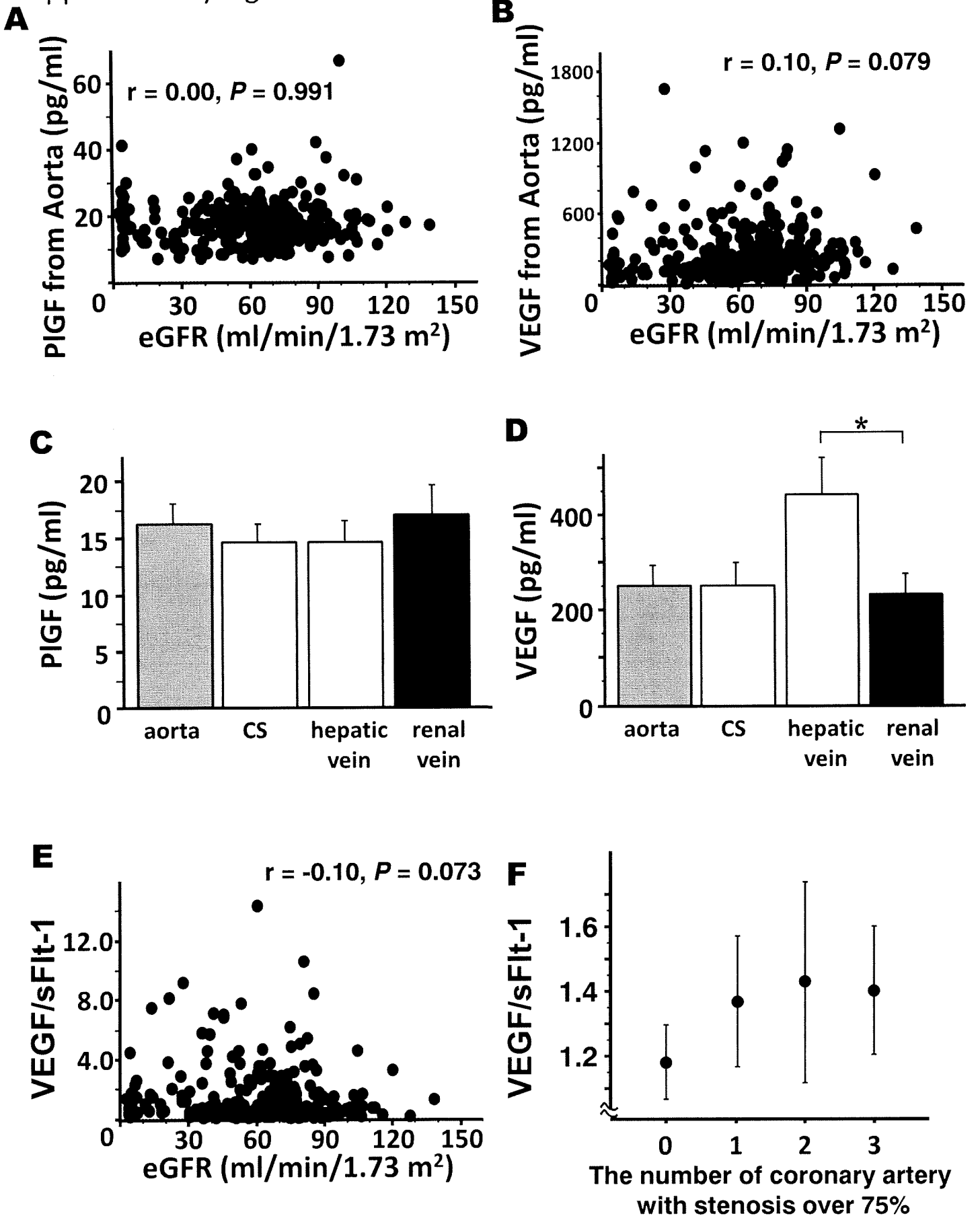

Supplementary Figure 4

Body weight (A) and blood pressure (B) of Apo-E KO mice in the experimental study. Temporal differences in body weight and blood pressure existed between the 4 groups, but the differences were diminished at the end of the experiments. Cont. PBS stands for control mice administered with PBS, cont. sFlt-1 control mice administered with sFlt-1, 5/6NR PBS 5/6 nephrectomized mice administered with PBS, 5/6 NR sFlt-1 5/6 nephrectomized mice administered with sFlt-1, respectively. $*P < 0.05$ between the 4 groups.
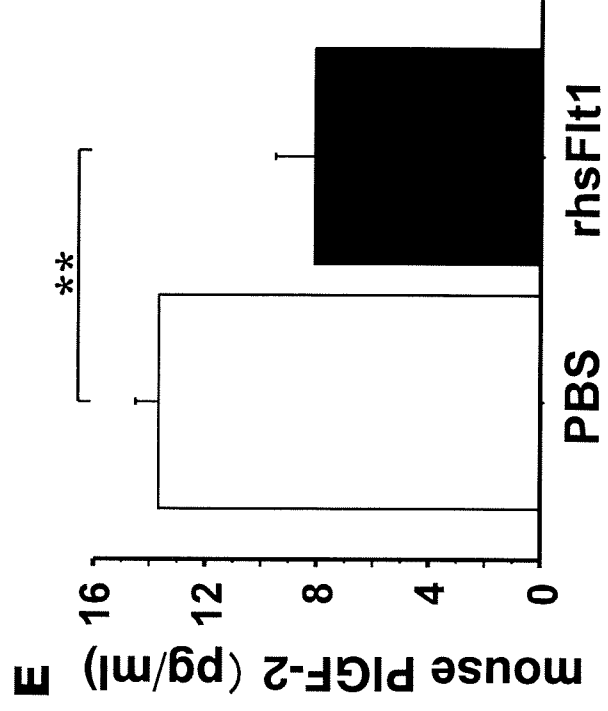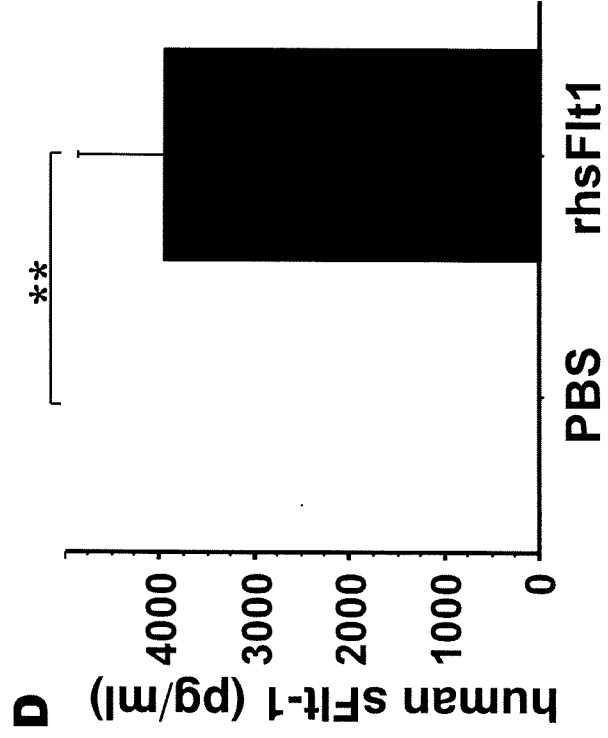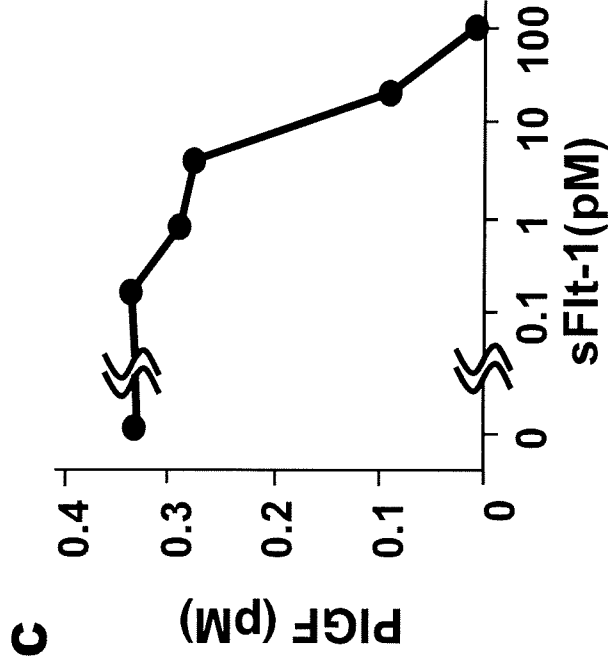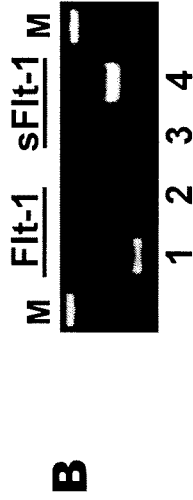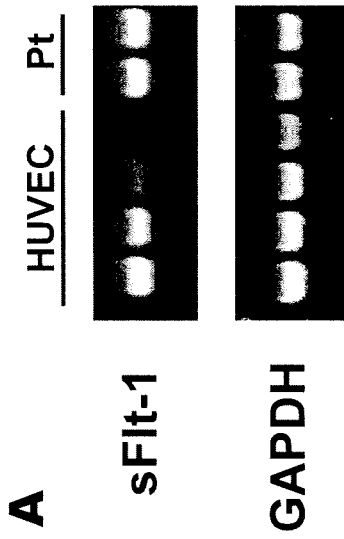
Supplemental References

1. Gensini GG. A more meaningful scoring system for determining the severity of coronary

heart disease. *Am. J. Cardiol.* 1983;51:606.

2. Krege, J.H., Hodgin, J.B., Hagaman, J.R., and Smithies, O. 1995. A noninvasive

computerized tail-cuff system for measuring blood pressure in mice. *Hypertension.*

25:1111-1115.

Supplementary Figure 1

A sFlt-1 (pg/ml) — aorta, CS, hepatic vein, renal vein

B sFlt-1 from Aorta (pg/ml) vs sFlt-1 from renal vein (pg/ml), r = 0.70, P < 0.001

C The number of coronary artery with stenosis over 75% vs Renal function group
1 (n=36) 2 (n=171) 3 (n=80) 4 (n=13) 5 (n=29)

D Gensini's Score vs Renal function group
1 (n=36) 2 (n=171) 3 (n=80) 4 (n=13) 5 (n=29)

E sFlt-1 (pg/ml) vs The number of coronary artery with stenosis over 75%

F PlGF (pg/ml) vs The number of coronary artery with stenosis over 75%

Supplementary Figure 2

A

r = 0.00, *P* = 0.991

PlGF from Aorta (pg/ml)

eGFR (ml/min/1.73 m²)

B

r = 0.10, *P* = 0.079

VEGF from Aorta (pg/ml)

eGFR (ml/min/1.73 m²)

C

PlGF (pg/ml)

aorta   CS   hepatic vein   renal vein

D

*

VEGF (pg/ml)

aorta   CS   hepatic vein   renal vein

E

r = -0.10, *P* = 0.073

VEGF/sFlt-1

eGFR (ml/min/1.73 m²)

F

VEGF/sFlt-1

The number of coronary artery with stenosis over 75%

Supplementary Figure 3

A

sFlt-1

GAPDH

HUVEC   Pt

B

M Flt-1   sFlt-1 M

1 2 3 4

C

PlGF (pM)

0.4
0.3
0.2
0.1
0

0   0.1   1   10   100

sFlt-1(pM)

D

human sFlt-1 (pg/ml)

4000
3000
2000
1000
0

**

PBS   rhsFlt1

E

mouse PlGF-2 (pg/ml)

16
12
8
4
0

**

PBS   rhsFlt1

Supplementary Figure 4

A

B

SBP

DBP

In vitro reprogramming of adult hepatocytes into insulin-producing cells without viral vectors

Hiroaki Motoyama [a], Shinichiro Ogawa [a,b,*], Atsushi Kubo [c], Shiro Miwa [a], Jun Nakayama [d], Yoh-ichi Tagawa [e,f], Shinichi Miyagawa [a]

[a] Department of Surgery, Shinshu University School of Medicine, 3-1-1 Asahi, Matsumoto, Nagano 390-8621, Japan
[b] McEwen Centre for Regenerative Medicine, University Health Network, 190 Elizabeth Street, Toronto, Ont., Canada M5G 2C4
[c] The First Department of Internal Medicine, Nara Medical University, 840, Shijo-cho, Kashihara, Nara 634-8522, Japan
[d] Department of Pathology, Shinshu University School of Medicine, 3-1-1 Asahi, Matsumoto, Nagano 390-8621, Japan
[e] Frontier Research Center, Tokyo Institute of Technology, 4259 Nagatsuta-cho, Midori-ku, Yokohama, Kanagawa 226-8503, Japan
[f] PRESTO, Japan Science & Technology Agency, 4-1-8 Honcho, Kawaguchi-shi, Saitama 332-0012, Japan

ARTICLE INFO

ABSTRACT

The pancreas and the liver share the same endodermal origin. We have been studying whether mature hepatocytes can be induced to differentiate into pancreatic β-cells by *in vitro* delivery of transcriptional factors using a non-viral approach. Here we showed that nucleofection allowed suitable transfection of primary hepatocytes employing various non-viral methods. We introduced either pancreatic and duodenal homeobox 1 (Pdx1) or neurogenin 3 (Ngn3), or both, into the mature cells using nucleofection. Co-expression of *pdx1* and *ngn3* using a bicistronic vector activated the transcription of various islet-related genes, and the transfected hepatocytes acquired the ability to synthesize and secrete insulin.

Our results suggest that simultaneous expression of Pdx1 and Ngn3 is an excellent inducer of liver-to-pancreas reprogramming, and that reprogramming will occur even in mature somatic cells without the need for viral vectors. These findings are of considerable significance for further therapeutic development for various intractable diseases including diabetes.

© 2009 Elsevier Inc. All rights reserved.

Introduction

In the process of embryogenesis, both the liver and ventral pancreas appear to arise from the same cell population located within the embryonic endoderm [1,2]. Focusing on this embryological homology, several groups have demonstrated that ectopic expression of key transcription factor genes for pancreas development in hepatic cells can induce them to differentiate into β-like cells [3,4]. Pancreatic and duodenal homeobox 1 (Pdx1), a member of the homeodomain-containing transcription factor family, plays an important role in initiating the differentiation of pancreatic endocrine cells. Ferber et al. were the first to report that transient adenovirus-mediated expression of *pdx1* in hepatocytes activated endogenous insulin expression and ameliorated hyperglycemia in mice with streptozotocin (STZ)-induced diabetes [5]. After this initial *in vivo* approach, many other studies [6,7] showed that several regulators of pancreas development, such as v-maf musculoapo-

neurotic fibrosarcoma oncogene homolog A (MafA), neurogenic differentiation 1 (NeuroD1), and neurogenin 3 (Ngn3) were potential inducers of islet cell differentiation in the liver. Although these transcription factors have an ability to induce the development of islet cells, it remains unclear whether the expression of a single gene alone, especially Pdx1, in hepatocytes is sufficient to induce reprogramming. In fact, it has been reported that *in vitro* induction of Pdx1 alone does not induce insulin production by mature hepatocytes, even though this is possible *in vivo* [5]. Kaneto et al. reported that adenoviral ectopic expression of Pdx1/VP16, a constitutively active form of Pdx1, together with Ngn3 or NeuroD, induced transcription of the insulin gene, resulting in amelioration of hyperglycemia in STZ mice, whereas this effect was mild when each gene was delivered independently [6]. These reports established that a suitable combination of transcription factors can activate target genes and act synergistically to induce insulin production in the liver.

On the other hand, several problems have been reported with the delivery of these transcriptional factors into liver cells using adenovirus-mediated strategies. Adenoviral vectors have hepatotoxicity caused by an immunological reaction in the liver [8]. To eliminate this reaction and to allow clinical application for the reprogramming of liver cells into an islet cell fate, a non-viral

* Corresponding author. Address: McEwen Centre for Regenerative Medicine, University Health Network, 190 Elizabeth Street, Toronto, Ont., Canada M5G 2C4. Fax: +1 416 595 5719.
E-mail addresses: sogawa@uhnresearch.ca, ogawash@shinshu-u.ac.jp (S. Ogawa).

approach for gene delivery is needed. However, no reports have indicated that pancreatic β-cells can be induced from mature hepatocytes *in vitro* by non-viral delivery of transcriptional factors.

In the present study, we demonstrated that nucleofection was effective for achieving transient expression of pancreatic transcriptional factors in mature hepatocytes. Furthermore, we showed that co-expression of *pdx1* and *ngn3* using a bicistronic expression approach activated the transcription of various islet-related genes including Ins1 and Ins2 in primary hepatocytes, and that the transfected cells acquired the ability to synthesize and secrete insulin. These results suggest that, if appropriate transcription factors can be transferred, reprogramming occurs even in mature somatic cells, and that the use of viral vectors is not indispensable for this approach.

Materials and methods

Plasmid construction. We generated three bicistronic plasmids: pCMV-Pdx1-IRES-EGFP (pCPIE), pCMV-Ngn3-IRES-DsRed (pCNID), and pCMV-Pdx1-IRES-Ngn3 (pCPIN) (Figs. 2A and 3A). The *pdx1* and *ngn3* cDNAs were PCR-amplified from the plasmids pZL1-Pdx1 (a generous gift from C. Wright) and pPdx1-IRES-Ngn3 (A.

Kubo, unpublished) using restriction site-attached primer sets, and cloned into the pIRES2-EGFP and pIRES2-DsRed (Clontech, Mountain View, CA), respectively. For construction of pCPIN, the Pdx1-IRES-Ngn3 fragment was excised from pPdx1-IRES-Ngn3 and cloned into pcDNA3.1 (Invitrogen, Carlsbad, CA). The details, including the PCR primer sets employed, are described in Supplementary Materials and Methods.

Cell preparation and culture. Hepatocytes were isolated from 6-week-old male C57Bl/6J mice (Clea Japan, Tokyo, Japan) by in situ collagenase perfusion, as described previously [9]. Cell viability measured by the trypan blue exclusion test was more than 95%.

βTC6 (American Type Culture Collection, Manassas, VA), a mouse insulinoma cell line [10], was used as a positive control. The conditions used for culture of these cells are described in Supplementary Materials and Methods.

Transfection with a non-viral procedure. Nucleofection of primary hepatocytes was performed according to the manufacturer's optimized protocol (Amaxa Biosystem, Cologne, Germany). Briefly, approximately 7×10^5 isolated hepatocytes were resuspended in 100 μL of mouse hepatocyte Nucleofector™ Solution, mixed with 6 μg of plasmid DNA, and pulsed with the program T-028. Fifteen minutes later, the cells were seeded at a density of $7 \times 10^4/cm^2$.
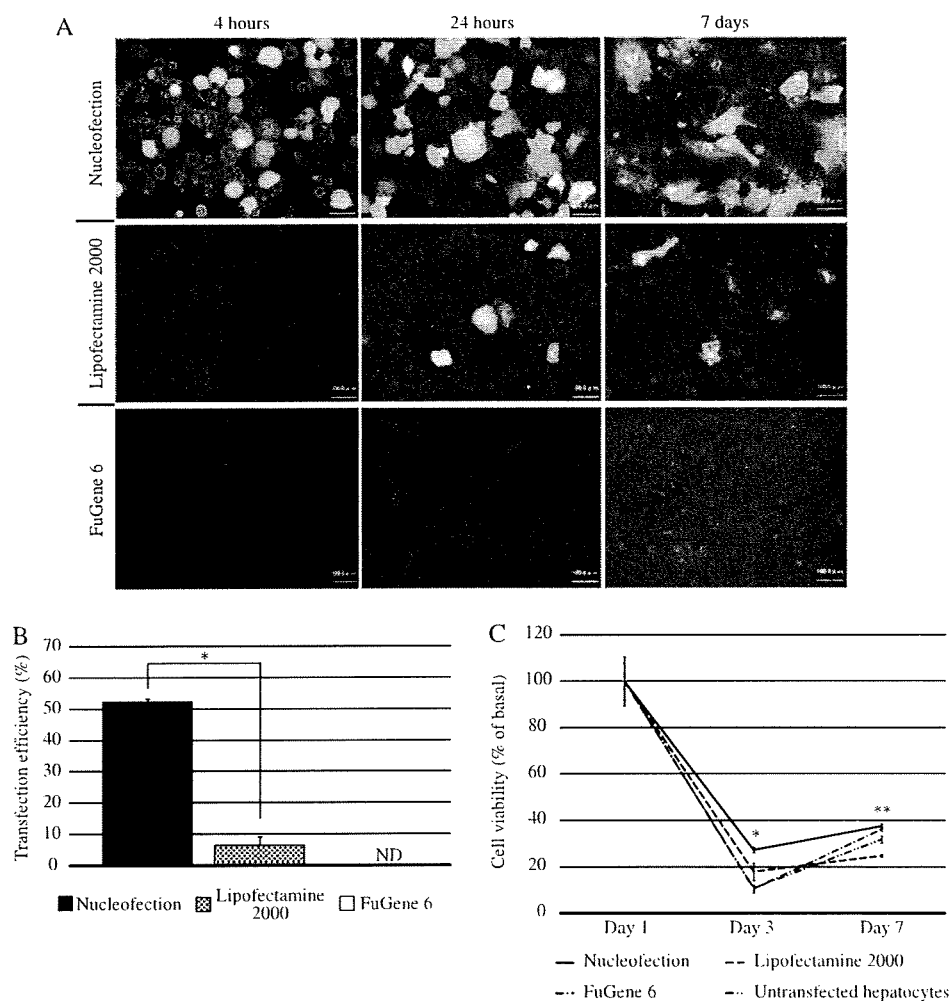

Fig. 1. Optimization of non-viral transfection procedures in primary cultured hepatocytes. (A) GFP expression in transfected hepatocytes. At 4 h after transfection, only the nucleofected hepatocytes expressed GFP. (B) Differential transfection efficiency of primary hepatocytes using three optimized DNA delivery methods. Data represent the mean ± standard deviation (SD) of the proportion of GFP-positive cells to the total number of cells. $P < 0.05$. ND, not detected. (C) Time-course analysis of both transfected and untransfected hepatocytes using the MTS assay. We compared the reduction of viability in each group at 3 and 7 days relative to that on day 1. P value < 0.05 relative to values for Lipofectamine 2000, FuGene 6 and untransfected hepatocytes ($n = 4$). P value < 0.05 relative to values for Lipofectamine 2000 and untransfected hepatocytes ($n = 4$).
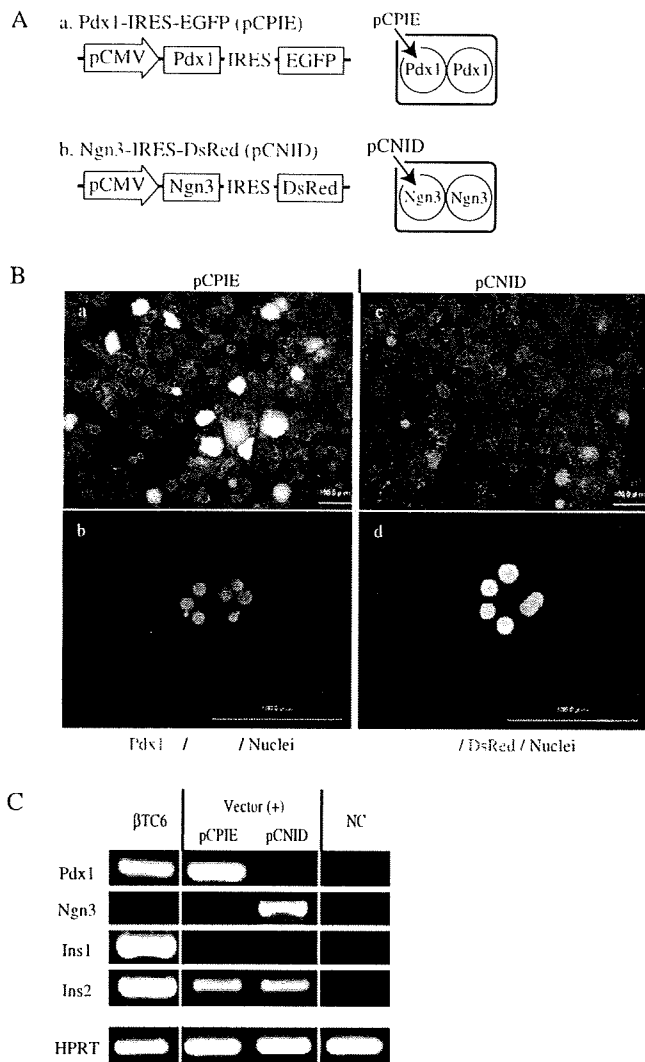
Fig. 2. Influence of ectopic expression of pdx1 and ngn3 alone. (A) Diagrams of bicistronic plasmids and schema of the transfection patterns. pCMV, cytomegalovirus promoter. IRES, internal ribosome entry site. (B) Live images and immunofluorescence staining of transfected hepatocytes. pCPIE-transfected hepatocytes expressed EGFP (a) and Pdx1 (b). pCNID-transfected hepatocytes also expressed DsRed (c) and Ngn3 (d). (C) Gene expression profiles of transfected cells. Plasmid-free nucleofected hepatocytes were prepared as a negative control (NC).

We compared the optimized nucleofection method with other non-viral transfection techniques such as Lipofectamine 2000 (Invitrogen) and FuGene 6 (Roche Applied Science, Mannheim, Germany). We performed initial optimization and transfection in accordance with the manufacturer's protocols, and prepared reagent-DNA complexes at ratios of 2.5:1 and 3:1, respectively.

To evaluate the efficiencies of the various techniques, we used the pmaxGFP plasmid, which encodes green fluorescent protein (GFP). The efficiency was determined as the proportion of GFP-positive cells to the total number of cells at 24 h by counting 30 fields at 200× magnification in three independent experiments.

Viability of transfected or untransfected hepatocytes was assessed by using CellTiter®96 AQueous One solution reagent (Promega, Madison, WI) with static incubation at 37 °C for 1 h, as recommended by the manufacturer.

RNA extraction and reverse transcription polymerase chain reaction analysis. Total RNA was extracted from 2- or 5-day-cultured hepatocytes using a Qiagen RNeasy mini kit (Qiagen) and treated with Turbo DNA free (Ambion, Austin, TX) to remove contaminating

genomic DNA. Two-microgram aliquots of total RNA were reverse-transcribed to cDNAs using Reverse transcription system (Promega) with an oligo-dT primer. Semi-quantitative reverse transcription polymerase chain reaction (RT-PCR) was performed as described previously [11]. The PCR primers are described in Supplementary Materials and Methods. Gene expression studies were repeated at least three times, and similar results were obtained.

Immunohistochemical analysis. Two-day-cultured hepatocytes were fixed with 4% paraformaldehyde/PBS for 20 min and then permeabilized with 0.1% Triton X/PBS for 10 min at room temperature. The fixed samples were incubated in Protein Block (DAKO, Carpentaria, CA) for 10 min at room temperature. They were then incubated with the primary antibody overnight at 4 °C and with the secondary antibody for 1 h in a humidified chamber. The antibodies used in this study are listed in Supplementary Materials and Methods. For nuclear staining, the cells were incubated for 5 min at room temperature with DAPI (4', 6-diamidino-2-phenylindole). The samples were then mounted in fluorescent mounting medium (DAKO) and observed using a BZ-8000 microscope (KEYENCE, Osaka, Japan).

Measurement of insulin and C-peptide in the cells and medium. Two-day-cultured hepatocytes were washed four times with PBS and then treated with acid–ethanol (0.18 M hydrochloric acid in 95% ethanol) at 4 °C overnight. The clear supernatants were used to assay the intracellular insulin and C-peptide contents, and the values obtained were normalized relative to the total protein content. The insulin and C-peptide contents were measured by an enzyme-linked immunosorbent assay (Insulin-ELISA kit, C-peptide-ELISA kit, Shibayagi, Gunma, Japan). Total protein content was measured by Protein Assay (Bio-Rad, Hercules, CA). Insulin secretion was measured using static incubation in Krebs-Ringer bicarbonate buffer (KRBB) supplemented with glucose, as described previously [12]. In brief, the cells were washed twice with KRBB containing 0.1% BSA (KRB-BSA). They were then preincubated for 1 h in KRB-BSA at 37 °C, and incubated for 2 h in KRB-BSA supplemented with 5 mM or 25 mM glucose, or without glucose. The concentration of the insulin secreted into the buffer solution was measured using an Insulin-ELISA kit as described above.

Statistical analysis. Values are expressed as the mean ± standard deviation (SD). Statistical significance was evaluated using Student's t test or one-way ANOVA (Bartlett's test and Scheffe's test) as necessary. Differences at $P < 0.05$ were considered to be statistically significant.

Results

Nucleofection allows high-efficiency transfection of primary mature hepatocytes

As a first step, we compared the transfection efficiencies of nucleofection with other non-viral transfection techniques, namely Lipofectamine 2000 and FuGene 6, using pmaxGFP. Transfection efficiency was determined as the percentage of GFP-positive cells among all vital cells at 24 h after transfection. Quantitative assessment revealed that transfection using nucleofection, Lipofectamine 2000 and FuGene 6 yielded 52.2 ± 3.7%, 6.3 ± 2.8% and 0% GFP-positive cells, respectively (Fig. 1A and B). GFP expression was maintained for 20 days, with a gradual decrease during that period. Cell viability was measured by MTS assay at 1, 3 and 7 days after transfection (Fig. 1C). The survival curves for each of the groups showed a similar pattern. However, the viability of nucleofected hepatocytes was significantly higher than for the other techniques. These results indicate that nucleofection is an efficient and suitable approach for gene transfer in primary hepatocytes, and accordingly in subsequent experiments we used nucleofection to achieve ectopic pancreatic gene expression in hepatocytes.
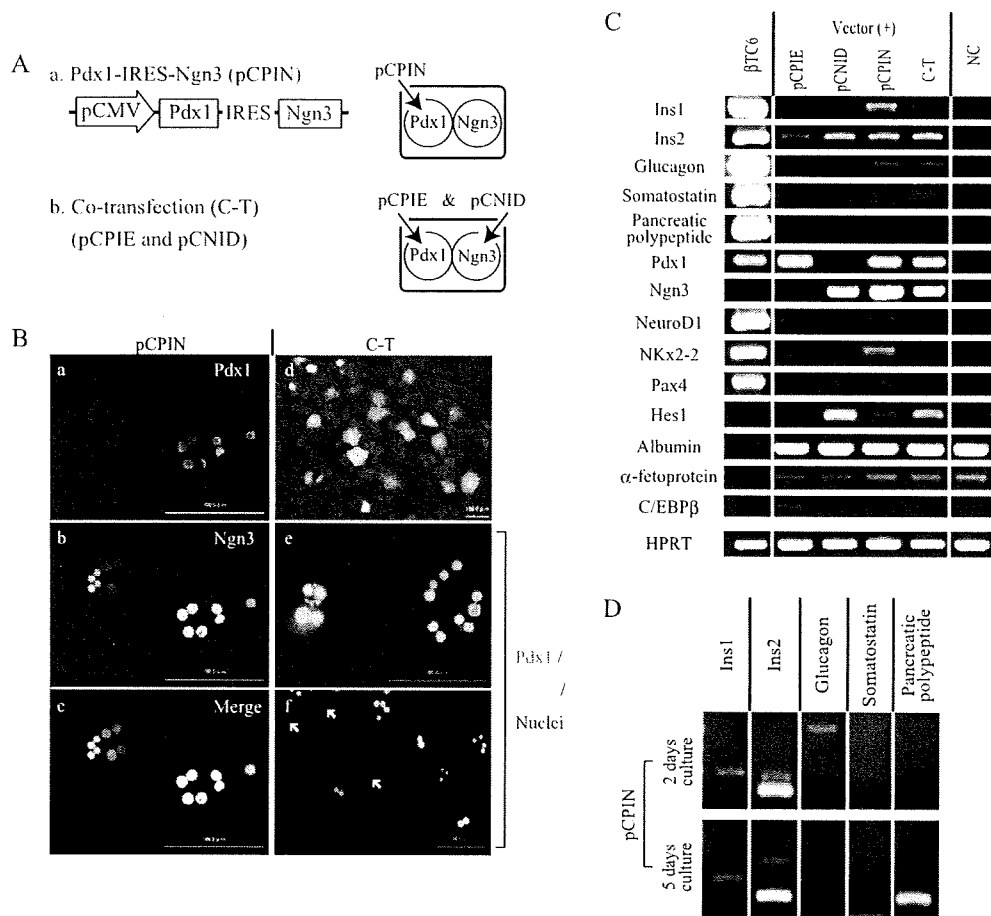
Fig. 3. Effects of co-expression of *pdx1* and *ngn3*. (A) Diagrams of bicistronic plasmids and schema of the transfection patterns. (B) Live images and immunofluorescence staining of transfected hepatocytes. In the C-T group, some of the co-transfected cells failed to coexpress Pdx1 and Ngn3 (arrow) (Fig. 3B-f). (C) Gene expression profiles of transfected hepatocytes. (D) Time-course analysis of gene expression in pCPIN-transfected hepatocytes.

Ecotpic expression of pdx1 or ngn3 alone is insufficient to induce reprogramming of mature hepatocytes

As an inducer of liver-to-pancreas reprogramming, we focused on two transcription factors, Pdx1 and Ngn3. Pdx1 is a master regulator of pancreas development, and Ngn3 is expressed in endocrine progenitors and is recognized as a key transcription factor for islet generation [13]. We constructed two IRES-dependent bicistronic expression plasmids, pCMV-Pdx1-IRES-EGFP (pCPIE) and pCMV-Ngn3-IRES-DsRed (pCNID) (Fig. 2A). When primary hepatocytes were transfected with these vectors, we detected the fluorescences of the corresponding EGFP or DsRed within 20 h after transfection (Fig. 2B-a and c). Immunofluorescence staining also demonstrated the expression of Pdx1 or Ngn3 (Fig. 2B-b and d). Western blotting detected the 47-kDa band of the Pdx1 protein and the 23-kDa band of the Ngn3 protein (data not shown). Transfection efficiencies were almost the same in case of pmaxGFP (45.5 ± 9.1% and 48.6 ± 6.1%, respectively). Next, to analyze the effect of ectopic gene expression, expression of the insulin gene was determined by semi-quantitative RT-PCR (Fig. 2C). In these hepatocytes, expression of insulin II (Ins2) was detected, but not insulin I (Ins1). The Ins2 gene is expressed in the developing brain and yolk sac as well as in pancreatic β-cells [14], whereas Ins1 gene expression is restricted to β-cells, suggesting that the expression of *pdx1* or *ngn3* alone is insufficient to induce specific reprogramming. Therefore we selected another strategy, co-expression of *pdx1* and *ngn3*.

Co-expression of pdx1 and ngn3 efficiently activates liver-to-pancreas reprogramming

To assess the effects of co-expression, we selected two approaches, namely bicistronic expression using IRES (pCPIN, pCMV-Pdx1-IRES-Ngn3) or independent co-transfection (C-T) (Fig. 3A). With IRES-dependent co-expression, the expression of Pdx1 and Ngn3 was mostly visualized in the same nucleus (Fig. 3B-a, b, c). However, in the C-T group, their expressions were observed independently, and co-localization was recognized in about 60.4 ± 16.0% of the transfected cells (Fig. 3B-d, e, f).

We analyzed further the molecular events occurring in nucleofected hepatocytes using semi-quantitive RT-PCR (Fig. 3C). Ins2 was expressed in all transfected hepatocytes, as was the case for sole expression of *pdx1* or *ngn3*. In contrast, expression of Ins1 was observed only in the pCPIN and C-T groups, in which both *pdx1* and *ngn3* were introduced. Glucagon was also expressed only in these groups. Somatostatin and pancreatic polypeptide were not detected in any of the transfected groups. In addition, we analyzed the expression of genes specific to the developing pancreas or liver. NeuroD1 was expressed in all of the transfected groups except negative control. On the other hand, expression of NK2 transcription factor-related locus 2 (Nkx2-2) and paired box gene 4 (Pax4) was restricted to the pCPIN group, in which Pdx1 and Ngn3 were expressed simultaneously. Hairy and enhancer of split 1 (Hes1), a negative regulator of Ngn3, was expressed in *ngn3*-overexpressing cells, and a similar result was obtained in the C-T group. Among li-

ver-specific genes, although expression of albumin and α-fetoprotein was retained in all groups, the expression of CCAAT/enhancer-binding protein β (C/EBPβ), whose suppression indicates hepatic dedifferentiation [15], was diminished only in the co-expressing groups. Furthermore, in the pCPIN group, the expression of Ins1 and Ins2 mRNA was maintained at 5 days after transfection when, interestingly, de novo expression of pancreatic polypeptide also appeared (Fig. 3D). These results suggest that nucleofection with the Pdx1 and Ngn3 bicistronic expression vector activated an endocrine reprogram in mature hepatocytes.

The bicistronic expression approach allows reprogramming to β-like cells

In order to confirm the production of endogenous insulin, we measured intracellular C-peptide levels in each of the transfected groups and compared them (Fig. 4A). Cells in which pdx1 or ngn3, or both, had been introduced showed significantly higher levels of C-peptide than plasmid-free transfected hepatocytes used as a negative control. In particular, the level of C-peptide in pCPIN-transfected cells was significantly higher than in other groups. The insulin content of the cells in the pCPIN-nucleofection group was also significantly (8-fold) higher than in the negative control (Fig. 4B). To test the functional ability of pCPIN-transfected hepatocytes, we quantified the glucose dependency of insulin secretion after treatment with 5 mM or 25 mM glucose using an insulin ELISA kit (Fig. 4C). The level of insulin secretion increased along with the glucose dose. These results indicated that hepatocytes simultaneously expressing Pdx1 and Ngn3 acquire characteristics similar to those of pancreatic β-cells.

Discussion

The reprogramming of hepatocytes into pancreatic β-cells would provide a renewable source for cell therapy in diabetic patients. Here we demonstrated that nucleofection is a very efficient system for introduction of foreign DNA into mature hapatocytes. Furthermore, we showed that mature hepatocytes can be reprogrammed to pancreatic fate by transient co-expression of pdx1 and ngn3. Using a bicistronic approach to introduce pdx1 and ngn3 into mature hepatocytes, we generated β-like cells that showed elevated cytoplasmic C-peptide content and insulin-secreting ability.

The Nucleofector™ technology is the first highly efficient non-viral gene transfer method that can be used for primary cells and cell lines that are difficult to transfect [16]. With a combination of specialized solutions and specific electrical parameters, this electroporation-based technology has beneficial features for transfection of slowly dividing cells such as primary cells, including hepatocytes. By using this method, we achieved a much higher transfection efficiency compared to other non-viral transfection procedures. Although the cell survival rate after gene delivery appeared to be relatively low, nucleofected hepatocytes showed higher viability in our experiments than untransfected cells (Fig. 1C). These results indicated that nucleofection is a suitable method for ex vivo gene transfer of primary hepatocytes, and that pre-transplant ex vivo nucleofection is a potentially useful technique for introducing selected transgenes without producing harmful effects.

Many attempts have been made to establish successful induction of islet neogenesis in the liver using viral-mediated delivery
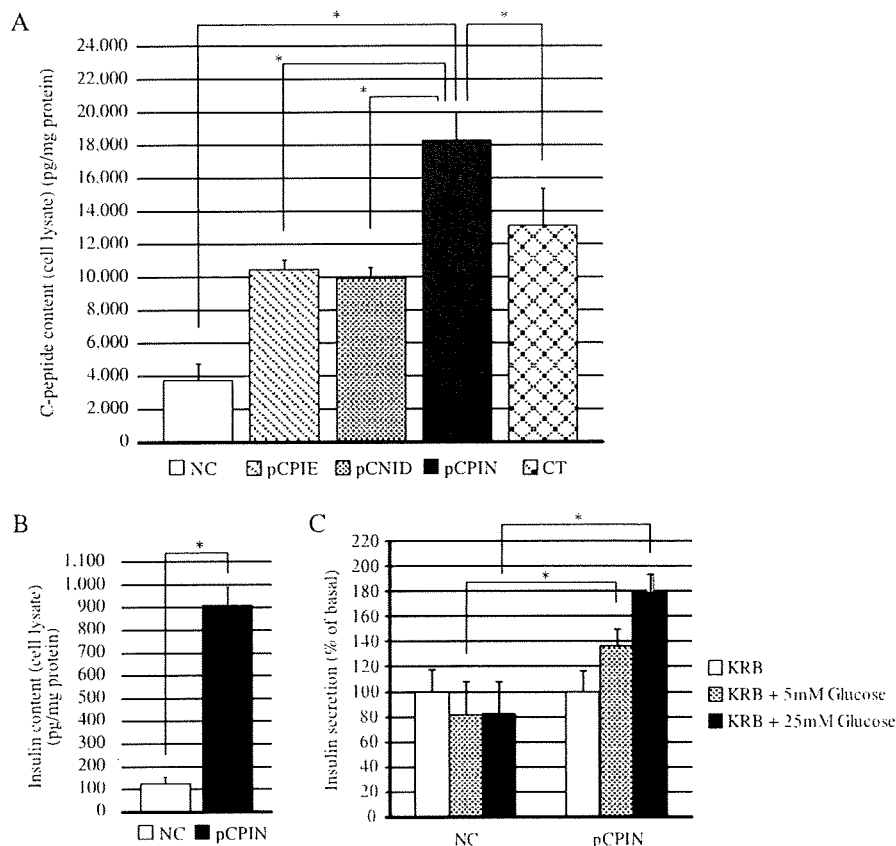

Fig. 4. Analysis of insulin biosynthesis and secretory ability. (A) Intracellular C-peptide content of transfected and untransfected hepatocytes (n = 3). The C-peptide levels in the negative control and transfection groups were assessed on day 2 after nucleofection. *P < 0.05. (B) Intracellular insulin content in the pCPIN and NC groups at 2 days of culture (n = 3). *P < 0.05. (C) Measurements of insulin secretion in the pCPIN and NC groups. Data represent the mean ± SD for three different experiments expressed as the percentage increase in insulin release relative to cells incubated in buffer without added glucose. *P value < 0.05 relative to NC incubated with 5 mM or 25 mM glucose.

of pancreatic transcriptional factors. Some studies investigating the effects of exogenous pancreatic transcriptional factors in the liver have demonstrated that Pdx1 alone was able to initiate, but not complete, the conversion process [6,7]. Consistent with those results, our data indicate that simultaneous induction of Pdx1, together with Ngn3, is necessary for reprogramming mature hepatocytes to an islet cell fate. More recently, it was shown that a small number of transcription factors can reprogram cultured adult skin cells into pluripotent stem (iPS) cells. Indeed, recent work on iPS cells suggests that a specific combination of multiple factors, instead of a single factor, might be the most effective way to reprogram adult cells. Melton et al. reported that a specific combination of three transcriptional factors (Ngn3, Pdx1 and MafA) can reprogram differentiated pancreatic exocrine cells in adult mice into cells that closely resemble β-cells using an adeno-viral delivery method [17]. This study showed that cellular reprogramming using defined factors might be feasible without reversion to a pluripotent stem cell state. Although it is not clear why these particular combinations are sufficient for adult β-cell reprogramming, we showed that a combination of *pdx1* and *ngn3* was able to directly reprogram hepatocytes into islet cells *in vitro* using non-viral methods. On the light of the results by Melton and colleagues [17], introduction of MafA in our vector might enhance the effect of reprogramming in our experiment. Although we have demonstrated the efficacy of a bicistronic approach using IRES, it has been reported that care should be taken with regard to the decreased capacity of IRES-dependent downstream gene expression [18], and therefore use of another multicistronic expression vector, such as the 2A segment of the foot-and-mouth disease virus [19], might be an interesting approach. Further investigation will be required to clarify the most suitable combinations of transcription factors for reprogramming mature hepatocytes into β-like cells.

In summary, simultaneous ectopic expression of Pdx1 and Ngn3 efficiently induces liver-to-pancreas reprogramming of mature hepatocytes, and the use of viral vectors is not indispensable for induction of such reprogramming in mature somatic cells. Our findings provide valuable information for the development of therapeutic strategies against various intractable diseases, including diabetes.

Acknowledgments

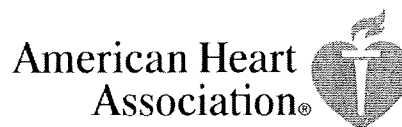## Appendix A. Supplementary data

Supplementary data associated with this article can be found, in the online version, at doi:10.1016/j.bbrc.2009.04.146.

References

[1] J.M. Rossi, N.R. Dunn, B.L. Hogan, K.S. Zaret, Distinct mesodermal signals, including BMPs from the septum transversum mesenchyme, are required in combination for hepatogenesis from the endoderm, Genes Dev. 15 (2001) 1998–2009.

[2] G. Deutsch, J. Jung, M. Zheng, J. Lora, K.S. Zaret, A bipotential precursor population for pancreas and liver within the embryonic endoderm, Development 128 (2001) 871–881.

[3] N. Nakajima-Nagata, T. Sakurai, T. Mitaka, T. Katakai, E. Yamato, J. Miyazaki, Y. Tabata, M. Sugai, A. Shimizu, In vitro induction of adult hepatic progenitor cells into insulin-producing cells, Biochem. Biophys. Res. Commun. 318 (2004) 625–630.

[4] H. Kawasaki, T. Mizuguchi, Y. Kikkawa, H. Oshima, Y. Sasaki, T. Tokino, Y. Kokai, J. Miyazaki, T. Katsuramaki, T. Mitaka, K. Hirata, In vitro transformation of adult rat hepatic progenitor cells into pancreatic endocrine hormone-producing cells, J. Hepatobiliary Pancreat. Surg. 15 (2008) 310–317.

[5] S. Ferber, A. Halkin, H. Cohen, I. Ber, Y. Einav, I. Goldberg, I. Barshack, R. Seijffers, J. Kopolovic, N. Kaiser, A. Karasik, Pancreatic and duodenal homeobox gene 1 induces expression of insulin genes in liver and ameliorates streptozotocin-induced hyperglycemia, Nat. Med. 6 (2000) 568–572.

[6] H. Kaneto, Y. Nakatani, T. Miyatsuka, T.A. Matsuoka, M. Matsuhisa, M. Hori, Y. Yamasaki, PDX-1/VP16 fusion protein, together with NeuroD or Ngn3, markedly induces insulin gene transcription and ameliorates glucose tolerance, Diabetes 54 (2005) 1009–1022.

[7] Y.D. Song, E.J. Lee, P. Yashar, L.E. Pfaff, S.Y. Kim, J.L. Jameson, Islet cell differentiation in liver by combinatorial expression of transcription factors neurogenin-3, BETA2, and RIPE3b1, Biochem. Biophys. Res. Commun. 354 (2007) 334–339.

[8] A.M. Gallo-Penn, P.S. Shirley, J.L. Andrews, S. Tinlin, S. Webster, C. Cameron, C. Hough, C. Notley, D. Lillicrap, M. Kaleko, S. Connelly, Systemic delivery of an adenoviral vector encoding canine factor VIII results in short-term phenotypic correction, inhibitor development, and biphasic liver toxicity in hemophilia A dogs, Blood 97 (2001) 107–113.

[9] M. Morita, Y. Watanabe, T. Akaike, Protective effect of hepatocyte growth factor on interferon-gamma-induced cytotoxicity in mouse hepatocytes, Hepatology 21 (1995) 1585–1593.

[10] S. Efrat, S. Linde, H. Kofod, D. Spector, M. Delannoy, S. Grant, D. Hanahan, S. Baekkeskov, Beta-cell lines derived from transgenic mice expressing a hybrid insulin gene-oncogene, Proc. Natl. Acad. Sci. USA 85 (1988) 9037–9041.

[11] S. Ogawa, Y. Tagawa, A. Kamiyoshi, A. Suzuki, J. Nakayama, Y. Hashikura, S. Miyagawa, Crucial roles of mesodermal cell lineages in a murine embryonic stem cell-derived in vitro liver organogenesis system, Stem Cells 23 (2005) 903–913.

[12] L. Le Brigand, A. Virsolvy, D. Manechez, J.J. Godfroid, B. Guardiola-Lemaitre, F.M. Gribble, F.M. Ashcroft, D. Bataille, In vitro mechanism of action on insulin release of S-22068, a new putative antidiabetic compound, Br. J. Pharmacol. 128 (1999) 1021–1026.

[13] C.S. Lee, N. Perreault, J.E. Brestelli, K.H. Kaestner, Neurogenin 3 is essential for the proper specification of gastric enteroendocrine cells and the maintenance of gastric epithelial cell identity, Genes Dev. 16 (2002) 1488–1497.

[14] L. Deltour, P. Leduque, N. Blume, O. Madsen, P. Dubois, J. Jami, D. Bucchini, Differential expression of the two nonallelic proinsulin genes in the developing mouse embryo, Proc. Natl. Acad. Sci. USA 90 (1993) 527–531.

[15] I. Meivar-Levy, T. Sapir, S. Gefen-Halevi, V. Aviv, I. Barshack, N. Onaca, E. Mor, S. Ferber, Pancreatic and duodenal homeobox gene 1 induces hepatic dedifferentiation by suppressing the expression of CCAAT/enhancer-binding protein beta, Hepatology 46 (2007) 898–905.

[16] O. Gresch, F.B. Engel, D. Nesic, T.T. Tran, H.M. England, E.S. Hickman, I. Korner, L. Gan, S. Chen, S. Castro-Obregon, R. Hammermann, J. Wolf, H. Muller-Hartmann, M. Nix, G. Siebenkotten, G. Kraus, K. Lun, New non-viral method for gene transfer into primary cells, Methods 33 (2004) 151–163.

[17] Q. Zhou, J. Brown, A. Kanarek, J. Rajagopal, D.A. Melton, In vivo reprogramming of adult pancreatic exocrine cells to beta-cells, Nature 455 (2008) 627–632.

[18] H. Mizuguchi, Z. Xu, A. Ishii-Watabe, E. Uchida, T. Hayakawa, IRES-dependent second gene expression is significantly lower than cap-dependent first gene expression in a bicistronic vector, Mol. Ther. 1 (2000) 376–382.

[19] K. Hasegawa, A.B. Cowan, N. Nakatsuji, H. Suemori, Efficient multicistronic expression of a transgene in human embryonic stem cells, Stem cells 25 (2007) 1707–1712.

Circulation Research

American Heart
Association®

*Learn and Live*₅ₘ

The online version of this article, along with updated information and services, is
located on the World Wide Web at:
http://circres.ahajournals.org/cgi/content/full/105/9/906

Data Supplement (unedited) at:
http://circres.ahajournals.org/cgi/content/full/CIRCRESAHA.109.199653/DC1

Periadventitial Adipose Tissue Plays a Critical Role in Vascular Remodeling

Minoru Takaoka, Daisuke Nagata, Shinji Kihara, Iichiro Shimomura, Yu Kimura, Yasuhiko Tabata, Yoshihiko Saito, Ryozo Nagai, Masataka Sata

Rationale: Obesity is associated with a high incidence of cardiovascular complications. However, the molecular link between obesity and vascular disease is not fully understood. Most previous studies have focused on the association between cardiovascular disease and accumulation of visceral fat. Periadventitial fat is distributed ubiquitously around arteries throughout the body.

Objective: Here, we investigated the impact of obesity on inflammation in the periadventitial adipose tissue and on lesion formation after vascular injury.

Methods and Results: High-fat, high-sucrose feeding induced inflammatory changes and decreased adiponectin expression in the periadventitial adipose tissue, which was associated with enhanced neointima formation after endovascular injury. Removal of periadventitial fat markedly enhanced neointima formation after injury, which was attenuated by transplantation of subcutaneous adipose tissue from mice fed on regular chow. Adiponectin-deficient mice showed markedly enhanced lesion formation, which was reversed by local delivery, but not systemic administration, of recombinant adiponectin to the periadventitial area. The conditioned medium from subcutaneous fat attenuated increased cell number of smooth muscle cells in response to platelet derived growth factor-BB.

Conclusions: Our findings suggest that periadventitial fat may protect against neointimal formation after angioplasty under physiological conditions and that inflammatory changes in the periadventitial fat may have a direct role in the pathogenesis of vascular disease accelerated by obesity. (*Circ Res.* 2009;105:906-911.)

Key Words: neointima ■ adipocyte ■ periadventitial tissue ■ smooth muscle cell ■ adipocytokine

O besity is a fast growing public health problem in industrialized countries[1-3] and is associated with cardiovascular complications.[4] Abdominal obesity is independently associated with cardiovascular disease, such as stroke, heart failure, and myocardial infarction.[5-9] Furthermore, recent reports suggest that obesity is an important risk factor for restenosis after percutaneous coronary intervention.[10]

It was reported that serum levels of circulating proinflammatory cytokines, such as tumor necrosis factor (TNF)-α, interleukin-6,[11] plasminogen activator inhibitor-1,[12] and monocyte chemoattractant protein-1,[13] are increased in overweight people with enhanced accumulation of visceral fat, whereas levels of antiinflammatory adipocytokines such as adiponectin (APN) are decreased.[14] In contrast to visceral fat, little attention has been paid to the role of periadventitial fat in vascular remodeling under physiological and pathological conditions. Periadventitial fat has been considered to mainly act a structural support for blood vessels.

Here, we investigated the effect of obesity on periadventitial adipose tissue and on lesion formation after vascular injury. Our findings support the idea that obesity induces changes in periadventitial tissue, which potentially affect lesion formation after vascular injury.

Methods

Animals

C57BL/6 mice were purchased from Japan SLC Inc (Shizuoka, Japan). APN-deficient mice (C57BL/6 background) have been described previously.[15] Green fluorescent protein (GFP) mice, which are transgenic mice (C57BL/6 background) that ubiquitously express enhanced GFP, were donated by Dr Masaru Okabe (Osaka University, Osaka, Japan).[16] All mice were backcrossed 10 times into a C57BL/6 background. To examine the effects of perivascular adipose tissue on injured arteries, neointimal hyperplasia in injured arteries was examined at 4 weeks after the vascular injury. Mice received standard chow diet (STD) or a high-fat high-sucrose diet (HF/HS) (45 kcal% fat, 20 wt% sucrose, D12451, Research Diets).

Circulation Research is available at http://circres.ahajournals.org   DOI: 10.1161/CIRCRESAHA.109.199653

All experimental procedures were approved by the University of Tokyo Ethics Committee for Animal Experiments and strictly adhered to the guidelines for animal experiments of the University of Tokyo.

Mouse Vascular Wire Injury

Vascular injury was induced as described previously.[17,18] To deliver APN into the perivascular area, recombinant mouse APN (5 μg per mouse; Wako Pure Chemical Industries Ltd) or PBS was administered using a gelatin hydrogel[19] for 4 weeks after vascular injury. Gelatin hydrogel was implanted on both the left and right femoral arteries at the same time as vascular injury. One artery received APN (APN gel group, n=6) and the other received PBS (PBS gel group, n=6). Other mice received recombinant mouse APN (5 μg per mouse) at the subcutaneous space (APN SC group, n=6) after wire-induced injury.

Transplantation of Adipose Tissue to Perivascular Area

Wire injury was performed with or without periadventitial adipose tissue. Then, 10 mg of visceral and subcutaneous fat tissues was harvested from the epididymis and flank, respectively. of wild-type (WT) mice fed a STD or HF/HS, lean GFP mice, or lean APN-deficient mice and implanted around the wire-injured femoral artery after removal of endogenous perivascular fat.

Quantification of Neointimal Hyperplasia

For morphometric studies, the femoral arteries were harvested 4 weeks after injury. Digitalized images were analyzed using image analysis software (Image J, NIH). The lumen, internal elastic lamina, and external elastic lamina were defined. The intimal (tissue between lumen and internal elastic lamina) and medial (tissue between internal elastic lamina and external elastic lamina) areas were recorded. Neointima/media area ratio was calculated.

Immunohistochemical Staining and Confocal Microscopic Observation

Paraffin-embedded sections (4 μm thick) were deparaffinized and blocked using 2% rabbit or horse serum. The sections were then incubated with anti-Mac3 antibody (BD Pharmingen). followed by incubation with avidin–biotin complex and Vector Red substrate (Vector Laboratories). Sections were counterstained with hematoxylin. To observe the GFP signal for histological analysis. the sections were then incubated with rabbit anti-GFP antibody (Molecular Probes) followed by Alexa Fluor 488–conjugated donkey anti-rabbit immunoglobulin antibody for immunohistochemical staining. The sections were observed under a confocal microscope (FLUOVIEW FV300, Olympus).

Measurement of Proinflammatory Cytokines

Total RNA was isolated from pooled perivascular adipose tissue (n=3 to 4 for each group) using a Qiagen RNeasy Minikit, after which, cDNA was generated using a RNA sample and a Quantitect Reverse Transcription kit (Qiagen). Real-time PCR was then carried out in an MxPro Mx3000P (Stratagene) using SYBR GREEN PCR Master Mix (TOYOBO). The following primers were used: 5'-GATG-GCAGAGATGGCACTCC-3' and 5'-CTTGCCAGTGCTGCCGTC-AT-3' for mouse APN; 5'-CCACTCACCTGCTGCTACTCAT-3' and 5'-TGGTGATCCTCTTGTAGCTCTCC-3' for mouse monocyte chemoattractant protein-1; 5'-TCCCAGGTTCTCTTCAAGGGA-3' and 5'-GGTGAGGAGCACGTAGTCGG-3' for mouse TNF-α; 5'-ACAACCACGGCCTTCCCTACTT-3' and 5'-CACGATTTCCCA-GAGAACATGTG-3' for mouse interleukin-6; 5'-TCAGCCC-TTGCTTGCCTCAT-3' and 5'-GCATAGCCAGCACCGAGGA-3' for mouse plasminogen activator inhibitor-1; and 5'-ATGACAA-CTTTGTCAAGCTCATTT-3' and 5'-GGTCCACCACCCTGTTGC-T-3' for GAPDH.

Non-standard Abbreviations and Acronyms	
APN	adiponectin
ca-AMPK	constitutively active AMPK
dn-AMPK	dominant negative AMP-activated protein kinase
GFP	green fluorescent protein
HF/HS	high-fat, high-sucrose
PDGF	platelet-derived growth factor
SMC	smooth muscle cell
STD	standard chow diet
TNF	tumor necrosis factor
WT	wild-type

Adipose Tissue Conditioned Medium

Visceral and subcutaneous fat tissues were harvested from the epididymis and flank, respectively, of lean or obese WT mice. Then, 400 mg of each sample was incubated at 37°C in 1 mL of DMEM medium containing 50 U/mL penicillin and 50 μg/mL streptomycin with 0.5% FBS for 4 hours.

Measurements of APN Protein Levels

APN concentration in the conditioned medium was measured using a mouse APN ELISA kit (Otsuka Pharmaceutical Co Ltd) according to the instructions of the manufacturer. The minimum detectable concentration of APN was 15.6 pg/mL.

Cell Culture

Rat vascular smooth muscle cells (SMCs) were seeded in 96-well plates at an initial density of 2×10^3 cells per well and allowed to attach for 24 hours. The cells were serum starved for 24 hours and then incubated with or without rat recombinant platelet-derived growth factor (PDGF)-BB (R&D Systems Inc) in the presence or absence of 100 μL/mL conditioned medium for 48 hours. Adenovirus vectors containing the gene for dominant negative AMP-activated protein kinase (dn-AMPK), constitutively active AMPK (ca-AMPK), and GFP were described previously.[20,21] SMCs were transduced with the indicated adenoviral vectors at a multiplicity of infection of 50 plaque-forming units for 24 hours before treatments. The number of cell in proliferation was determined by MTS assay using CellTiter 96 Aqueous One Solution Cell Proliferation Assay (Promega).

Statistical Analysis

All results are expressed as means±SEM. Differences between groups were evaluated for statistical significance using Student t test. Values of $P < 0.05$ were considered significant.

Results

To investigate the effect of obesity on lesion formation after vascular injury, 6-week-old C57BL6 mice were fed STD or HF/HS diet for 16 weeks. The HF/HS mice increased body weight by ≈54% (STD, 25.4±0.1 g; HF/HS, 39.0±2.2 g). Histological studies demonstrated abundant macrophage infiltration in adventitial adipose tissue as determined by anti-Mac3 immunostaining (Figure 1A). Consistent with these changes, quantitative RT-PCR analysis revealed that APN expression was downregulated with upregulation of proinflammatory cytokines within the periadventitial fat of HF/HS mice (Figure 1B). We inserted a wire into the femoral artery of STD and HF/HS mice.[17,18] At 4 weeks after the
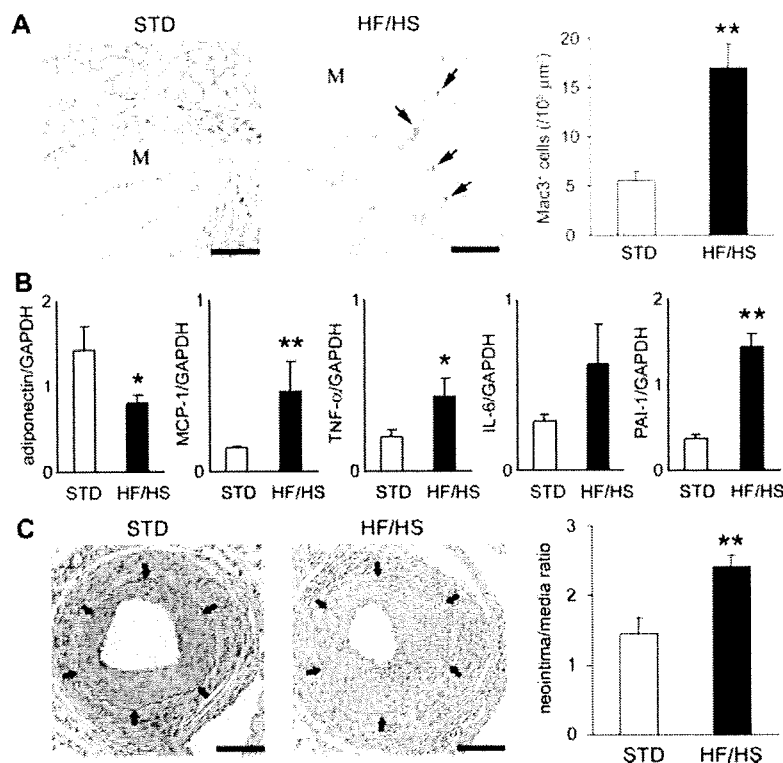
Figure 1. Obesity-induced inflammatory changes in periadventitial fat and enhanced neointimal hyperplasia. A, Obesity-induced accumulation of inflammatory cells in periadventitial fat. Immuno-histochemical analysis showed accumulation of Mac3-positive macrophages (arrows) within peri-adventitial fat in obese mice. Scale bar: 50 μm. Results are expressed as means±SEM. **P<0.01. M indicates media of femoral artery. B, Expression of mRNA in periadventitial fat around femoral artery from STD (n=6) and HF/HS (n=6) WT C57BL6 mice. Expression level was assessed by real-time PCR normalized to each GAPDH level. Results are expressed as means±SEM. *P<0.05, **P<0.01. C, Hematoxylin/eosin-stained sections of femoral arteries from mice fed on STD or HF/HS diet 4 weeks after endovascular injury. Arrows indicate internal elastic lamina. Scale bar: 100 μm. Morphometric analysis of injured femoral arteries in lean (n=7) and obese (n=6) mice 4 weeks after wire-induced injury. Results are expressed as means±SEM. **P<0.01.

injury, intimal hyperplasia was enhanced in HF/HS mice compared to that in STD mice (P<0.01) (Figure 1C).

To investigate the impact of the phenotypic changes in periadventitial adipose tissue on vascular remodeling after injury, we replaced the periadventitial adipose tissue with exogenous fat after insertion of the wire. First, the periadventitial fat tissue around the femoral artery was carefully removed and the artery was injured. Then, subcutaneous fat from a GFP mouse was transplanted around the injured artery. Histological analysis showed the presence of GFP-positive adipocytes in close proximity to the injured artery at 1 week and 4 weeks after transplantation (Figure 2A), indicating that the transplanted fat attached and survived around the artery. There was no statistical difference between subcutaneous fat and visceral fat in the efficiency of grafting, as determined by immunofluorescence staining of the cross-section at 4 weeks after the grafting. Fat transplantation induced neovascularization around the artery (Online Figure I, available in the Online Data Supplement at http://circres.ahajournals.org). Morphometric analysis revealed that neointimal hyperplasia was markedly enhanced by removal of periadventitial fat in STD mice (Figure 2B). Transplantation of subcutaneous fat from STD mice markedly attenuated the neointima (Figure 2C), suggesting that perivascular adipose tissue may have a protective role in neointimal hyperplasia in STD mice. Atheroprotective effect of exogenous fat tissue was not observed when subcutaneous fat from HF/HS mice or visceral fat was transplanted (Figure 2C, Online Figure II).

To analyze which molecule in periadventitial fat contributes to the attenuation of lesion formation in STD mice, we focused on APN. Consistent with a previous report,[22] APN-deficient mice showed severe neointimal thickening and increased proliferation of vascular SMCs in response to

vascular injury, compared with C57BL6 WT mice (P<0.05) (Figure 3A and 3B). To investigate the local effects of periadventitial fat APN on vascular remodeling, recombinant APN was delivered locally to the adventitial space in APN-deficient mice, using gelatin hydrogel.[19] Gelatin hydrogel filled with APN or PBS was transplanted into the periadventitial area. Four weeks after endovascular injury, perivascular delivery of APN to the femoral artery reduced endovascular injury-induced neointimal hyperplasia compared with that in the PBS-delivered artery in APN-deficient mice (P<0.001) (Figure 3C). These findings indicate that APN secreted from periadventitial fat has a protective role in lesion formation in response to endovascular injury.

Next, we investigated the effects of humoral factors secreted from fat tissue on SMCs proliferation in vitro. The conditioned medium from the subcutaneous fat of STD mice, but not of HF/HS mice, attenuated increased SMC numbers induced by PDGF-BB (P=0.05) (Figure 4A). The conditioned medium of HF/HS fat increased SMC numbers (P=0.001). RT-PCR analysis revealed that proinflammatory cytokine expression was upregulated in the HF/HS fat than STD fat (Online Figure III). Pretreatment with a neutralizing anti–TNF-α antibody suppressed the increased SMC numbers (P=0.05). Furthermore, the conditioned medium from the subcutaneous fat of APN-deficient mice increased SMC numbers compared with conditioned medium from STD subcutaneous fat (P=0.05) (Figure 4A). We measured APN level in the conditioned medium from the subcutaneous fat of STD and HF/HS mice using an ELISA kit. APN protein levels were significantly higher in the conditioned medium from STD mice than in that from HF/HS mice (P=0.01) (Figure 4B). These results showed that inflammatory cytokines such as TNF-α secreted from fat increased SMC
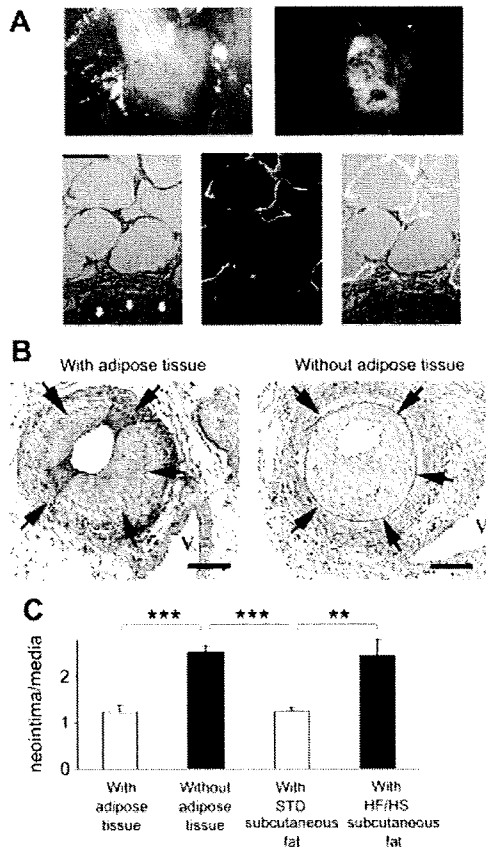
A

B

With adipose tissue   Without adipose tissue

C

Figure 2. Transplantation of subcutaneous fat from STD mice attenuated lesion formation after removal of perivascular adipose tissue. A, Subcutaneous adipose tissue from GFP-mice fed on STD was implanted around the injured artery of WT mice after removal of perivascular adipose tissue. At 1 week, the injured artery (top left) was illuminated with a GFP-lighting system (Illumatool Tunable Lighting System, LT-9800, Lightools Research, Encinitas, Calif) and observed using a cooled charge-coupled device camera (VB-6010, Keyence, Osaka) (top right). Immunofluorescent staining showed that GFP-positive (green) transplanted adipose tissue was present 1 week after wire-induced endovascular injury (bottom images). Arrows indicate external elastic lamina of injured artery. Scale bar: 25 μm. Left, Differential interference contrast image. Middle, GFP signal. Right, Merged. B, Representative hematoxylin/eosin-stained sections of femoral arteries at 4 weeks after endovascular injury with or without adipose tissue in STD WT mice. Arrows indicate internal elastic lamina. Scale bar: 100 μm. C, Morphometric analysis of injured femoral arteries with (n=6) or without (n=5) adipose tissue at 4 weeks. Subcutaneous fat from STD (n=6) or HF/HD (n=6) mice was transplanted after removal of endogenous periadventitial adipose tissue. Results are expressed as means±SEM. **$P<0.01$, ***$P<0.001$.

numbers and that APN secreted from fat suppressed SMC numbers in response to PDGF-BB stimulation. These findings indicate that humoral factors secreted from adipose tissues play a crucial role in regulation of SMCs proliferation.

To investigate the mechanism by which APN modified SMCs number cultured with PDGF-BB, we stimulated cultured SMCs with PDGF-BB in the presence or absence of APN. APN suppressed the increased SMC number induced by PDGF-BB ($P=0.01$) but had no effect on SMCs number in the absence of PDGF-BB (Figure 5). To test whether AMPK signaling was involved in the action of APN, we pretreated SMCs with adenoviral vector expressing dn-AMPK or ca-
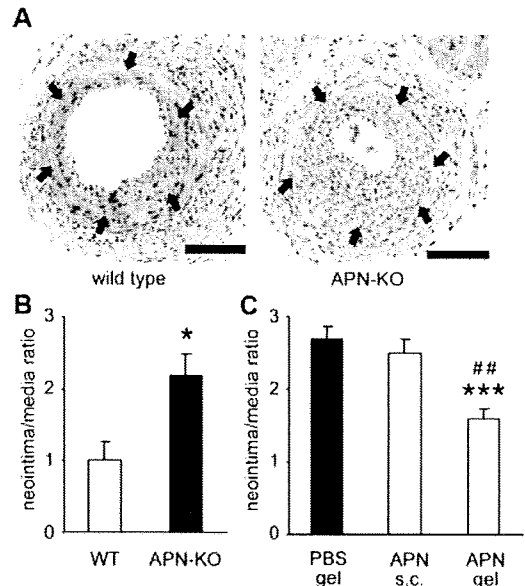
A

wild type   APN-KO

B   **C**

WT   APN-KO   PBS   APN   APN
gel   s.c.   gel

Figure 3. APN-secreted from periadventitial adipose tissue plays a protective role in neointima formation after endovascular injury. A, Hematoxylin/eosin-stained sections of femoral arteries from WT mice and APN-deficient (APN-KO) mice harvested 4 weeks after injury. Arrows indicate internal elastic lamina. Scale bar: 100 μm. B, Morphometric analysis of injured femoral arteries from WT (n=5) and APN-KO (n=5) mice 4 weeks after wire-induced injury. Results are expressed as means±SEM. *$P<0.05$. C, Effect of perivascular APN administration on neointima formation in APN-KO mice. Morphometric analysis of injured femoral arteries in APN-KO mice treated with PBS gel (n=6), subcutaneous injection of APN (APN s.c.) (n=6), and APN gel (n=6) 4 weeks after wire-induced injury. Results are expressed as means±SEM. ***$P<0.001$ compared with PBS gel; ##$P<0.01$ compared with APN s.c.

AMPK. Transduction with dn-AMPK abrogated the suppressive effects of APN on the increased SMCs number induced by PDGF-BB. On the other hand, ca-AMPK suppressed increased SMCs number induced by PDGF-BB ($P=0.05$) (Figure 5). These results indicated that AMPK mediates suppressive effect of APN on the PDGF-BB-induced increased SMCs number.

Discussion

In this study, we investigated the effect of obesity on inflammation in periadventitial adipose tissue and on lesion formation after vascular injury. Obesity-induced inflammation in periadventitial adipose tissue, with upregulation of inflammatory adipocytokines and downregulation of the antiinflammatory adipocytokine APN. These changes were associated with enhanced neointima formation after endovascular injury. Obesity-induced enhancement of lesion formation was attenuated by replacement of periadventitial adipose tissue with exogenous subcutaneous fat. Our findings suggest that obesity causes inflammatory changes and downregulation of APN in the periadventitial adipose tissue, which potentially influence lesion formation after vascular injury.

Endothelial injury induces adhesion and migration of leukocytes, macrophages, and bone marrow–derived progenitor cells into the artery wall.[16,23] It is well known that proinflammatory cytokines have a fundamental role in medi-